Extending Operational Zone of Rotary Power Flow Controller by Controlling Tap-Changers of Transformers

M. Tolue Khayami*(C.A.) and H. A. Shayanfar**

Abstract: This paper proposes a method for extending the ability of Rotary Power Flow Controller (RPFC) using tap-changer of the RPFC's transformers. A detailed model of the device is presented to analyze the effects of the tap changer operation on the performance of the RPFC. To evaluate the results, the RPFC model is simulated using PSCAD/EMTDC software. Dynamic operation of the RPFC on a 400 kV transmission line is studied. Based on the results, using tap-changer of transformers can extend the RPFC ability to control the active power of the transmission line about 25%.

Keywords: Active Power Control, Dynamic Stability, Rotary Phase Shifting Transformer, Rotary Power Flow Controller (RPFC), Tap-Changing Transformer.

1 Introduction

Power flow control is important in the steady state and dynamic operation of an interconnected power system. In its general form, power flows through the network are mainly determined by the magnitude and phase angle of transmission line voltage and impedance. Transmission lines with lower impedance take a more share of power flows than those with higher impedance [1]. However, Flexible AC Transmission Systems (FACTS) devices such as Unified Power Flow Controller (UPFC) and rotary power flow controller (RPFC)can control power flow of a transmission line according to the operator command. Moreover, FACTS devices can increase capacity, flexibility and controllability of the electric transmission network [1-4].

For the first time, in 1998 the RPFC concept was presented based on Rotary Phase Shifting Transformer (RPST) structure [5, 6]. The RPFC can balance active power flow in a parallel transmission corridor in normal and contingency conditions [7, 8].

The RPFC performance is similar to UPFC. The high power semiconductor switches of the UPFC increase the dynamic response speed. The disadvantages of these switches are high cost and low reliability. Therefore, UPFC has higher cost and lower reliability compared to devices consisting transformer and rotating machinery components such as RPFC. Operation and maintenance costs of the RPFC are lower than UPFC. Therefore, using the RPFC for expanding the transmission line capability and power flow control is more economic than installation of the UPFC or building new lines [9, 10].

A dynamic model for double shaft RPFC is presented in [7]. The shunt and series branch are modeled using current and voltage sources. The transformers and RPSTs magnetizing inductances are neglected.

Based on the model presented in [7], the performance of RPFC for controlling the power flow in a transmission corridor is simulated in [8]. Moreover, the influence of the RPST number of poles on the RPFC performances is studied. It is shown that the utilization of the RPFC allows more flexible control of power flow in normal and contingency conditions.

The remaining researches are focused on single-shaft RPFC. An approximate dynamic model for single-shaft RPFC is presented and the effects of transformers voltage ratio and the angle between rotor and stator of the RPSTs are analyzed. The dynamic performance of the RPFC during faults and other switching operations has been studied [10]. Potential advantages of RPFC are: (a) continuous adjustment of transmission line voltage phase shift, (b) longer thermal time constants than power electronic based devices, (c) consistency with other transmission equipment such as transformers, (d) absence of harmonics and generator interaction issues associated with power electronic based devices, and (e) reliable operation during network transients [11, 12].

Iranian Journal of Electrical & Electronic Engineering, 2014.
Paper first received 04 Aug. 2013 and in revised form 25 Feb. 2014.
* The Author is with the Department of Electrical Engineering, Science and Research Branch, Islamic Azad University, Tehran, Iran.
** The Author is with Center of Excellence for Power System Automation and Operation, Department of Electrical Engineering, Iran University of Science & Technology, Tehran, Iran.
Emails: moh.tolue@gmail.com and hashayanfar@gmail.com.

Performance specification, operational zone and active and reactive power coupling of the RPFC are evaluated based on the device steady state model [13, 14]. Allocation of the RPFC in a high voltage 400 kV transmission network for improving loading and voltage security indices and reliability is presented in [15] and [16].

In this paper, the results of the series and shunt transformers tap-changers operation on the performance of the RPFC are analyzed. Transmission transformers usually have tab-changer installed on them. In the transmission system, tab-changers changes by load. Therefore, we have assumed that RPFC transformers already have tap-changer mechanism installed on them and we suggest using them to extend the operational zone. Therefore no extra cost will be added to the system. The active and reactive power flow control zones, dynamic and steady state operation of the RPFC with and without tap-changing transformers are studied. Moreover, the effects of RPST's magnetizing inductance have been considered, because the effect of magnetizing branch is not negligible in rotary machines - in contrast to transformers - as the air gap between rotor and stator is wide and the machine has large magnetizing currents. This inductance has been neglected in all other references. The coupling between the consumed reactive and active power passed through the RPFC is presented. Using detailed mathematical model and simulation of precise model in PSCAD/EMTDC software environment, comparison has been made between dynamic and steady state operation of the RPFC with and without tap-changing transformers. The extension of the operational zone of the RPFC due to the proposed structure is evaluated using analytical and simulation results.

The RPFC configuration is introduced in Section 2. In Section 3 a precise model for RPFC is presented. Based on this model, the active and reactive power variation and dependency are evaluated. The comparison between operation of the RPFC with and without tap-changing transformers is presented in Section 4. A 400 kV test line is simulated and the results are described in Section 5. Finally, Section 6 concludes the results of paper.

2 RPFC Structure

The configuration of the RPFC is shown in Fig. 1. A shunt transformer connects the rotor of the RPSTs and the network. The stators of both RPSTs are connected in series with the series transformer. This transformer injects controllable voltage into the grid. In the proposed RPFC the tap-changing series and shunt are utilized to extend the operation region. A double-shaft RPFC is proposed. Therefore, the angle between the stator and the rotor of each RPST can be controlled independently.

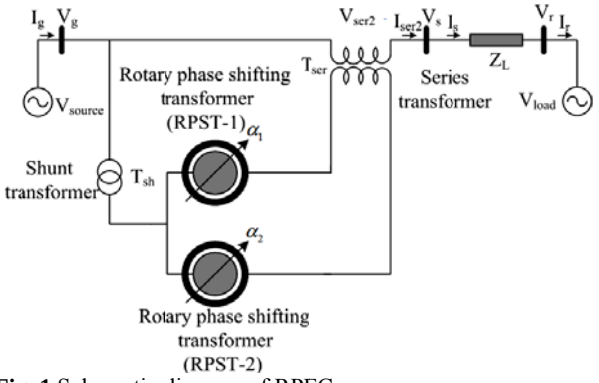

Fig. 1 Schematic diagram of RPFC.

3 RPFC Modeling

By using the RPFC equivalent circuit and considering the active and reactive power losses, the device equations are presented in this section.

3.1 Relations between RPFC Components

The RPFC equivalent circuit is depicted in Fig. 2. For the shunt transformer we have:

$$\overline{V}_{sh_1} = T_{sh}.e^{j\gamma}(\overline{V}_{sh_2} + Z_{sh}.I_{sh_2}) \quad (1)$$

$$\bar{I}_{sh_1} = \frac{1}{T_{sh}.e^{j\gamma}}.\bar{I}_{sh_2} \quad (2)$$

where, $\overline{V}_{sh1}$ and $\overline{V}_{sh2}$ are the shunt transformer primary and secondary voltages, T_{sh} is the shunt transformer turns ratio, Z_{sh} is equivalent impedance of shunt transformer and γ is the phase difference between $\overline{V}_{sh1}$ and $\overline{V}_{sh2}$. Supposing the tap-changer capability to change the voltage up to ±10%, we can write:

$$0.9T_{sh-n} < T_{sh} < 1.1T_{sh-n} \quad (3)$$

where, $T_{sh\text{-}n}$ is the nominal turn's ratio of the shunt transformer. By denoting T_{rpst1} and T_{rpst2} as the RPSTs turns ratio, α_1 and α_2 the phase difference between the rotor and stator of the two RPSTs and Z_{rt1}, Z_{rt2} equivalent impedances of RPSTs, following relations between the primary and secondary voltages and currents can be written as:

$$\overline{V}_{sh_2} = T_{rpst_1}.e^{j\alpha_1}(\overline{V}_{s_1} + Z_{rt_1}.I_{ser_1}) \quad (4)$$

$$\bar{I}_{R1} = \frac{1}{T_{rpst1}}e^{-j\alpha_1}.\bar{I}_{ser1} + I_{o1} \quad (5)$$

and

$$\overline{V}_{sh_2} = T_{rpst_2}.e^{j\alpha_2}(\overline{V}_{s_2} - Z_{rt_2}.I_{ser_1}) \quad (6)$$

$$\bar{I}_{R2} = -\frac{1}{T_{rpst2}}e^{-j\alpha_2}.\bar{I}_{ser1} + I_{o2} \quad (7)$$

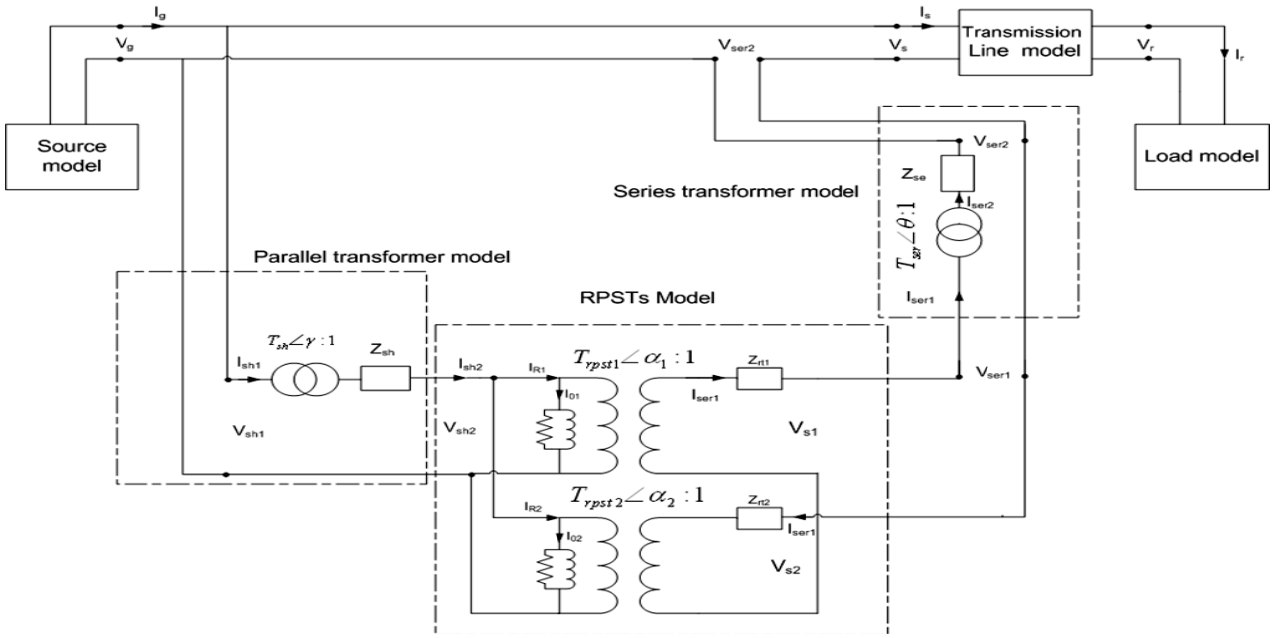

Fig. 2 Equivalent circuit of RPFC.

Supposing θ the phase difference between the series transformer primary and secondary voltages (V_{ser1} and V_{ser2}), I_{o1} and I_{o2} are magnetizing current of the RPSTs, T_{ser} its turn's ratio and Z_{se} is the equivalent impedance of the series transformer, we have:

$$\overline{V}_{ser_1} = T_{ser}.e^{j\theta}(\overline{V}_{ser_2} + Z_{se}.I_{ser_2}) \tag{8}$$

$$\bar{I}_{ser1} = \frac{1}{T_{ser}} e^{-j\theta}.\bar{I}_{ser2} \tag{9}$$

Operation of the series transformer tap-changer alters the turn's ratio, i.e.:

$$0.9T_{ser-n} < T_{ser} < 1.1T_{ser-n} \tag{10}$$

where, $T_{ser\text{-}n}$ is the nominal turn's ratio of the series transformer. The tap-changer is proposed for the HV side of the transformer.

3.2 Injected Voltage

The voltage injected into the line ($\overline{V}_{ser\,2}$) can be calculated by the following equation:

$$\overline{V}_{ser\,1} = \overline{V}_{s1} - \overline{V}_{s2} \tag{11}$$

Substituting Eqs. (4) and (6) into Eq. (11), we have:

$$\overline{V}_{ser_1} = (\frac{e^{-j\alpha_1}}{T_{rpst1}} - \frac{e^{-j\alpha_2}}{T_{rpst2}})\overline{V}_{sh_2} - \left(Z_{rt_1} + Z_{rt_2}\right)I_{ser_1} \tag{12}$$

Substituting $\overline{V}_{sh2}$ from Eq. (1) into Eq. (12), we have:

$$\begin{aligned}\overline{V}_{ser_1} &= \frac{1}{T_{sh}.e^{j\gamma}}(\frac{e^{-j\alpha_1}}{T_{rpst1}} - \frac{e^{-j\alpha_2}}{T_{rpst2}})\overline{V}_{sh_1} \\ &- \left(Z_{rt_1} + Z_{rt_2}\right).I_{ser_1} \\ &-(\frac{e^{-j\alpha_1}}{T_{rpst1}} - \frac{e^{-j\alpha_2}}{T_{rpst2}}).Z_{sh}.I_{sh_2}\end{aligned} \tag{13}$$

If $Z_{rt_1} = Z_{rt_2} = Z_{rt}$, from Eqs. (8) and (13) we have:

$$\begin{aligned}\overline{V}_{ser2} &= \frac{1}{T_{sh}.T_{ser}}(\frac{e^{-j\alpha_1}}{T_{rpst1}} - \frac{e^{-j\alpha_2}}{T_{rpst2}})e^{-j(\theta+\gamma)}\overline{V}_{sh1} \\ &-\frac{1}{T_{ser}e^{j\theta}}.2.Z_{rt}.I_{ser_1} \\ &-\frac{1}{T_{ser}.e^{j\theta}}(\frac{e^{-j\alpha_1}}{T_{rpst1}} - \frac{e^{-j\alpha_2}}{T_{rpst2}}).Z_{sh}.I_{sh_2} - Z_{se}.I_{ser_2}\end{aligned} \tag{14}$$

Supposing $I_{o_1} = I_{o_2} = I_o$, the current injected into the RPSTs (I_{sh2}) can be calculated by the following equation:

$$\begin{aligned}I_{sh_2} &= I_{R_1} + I_{R_2} = (\frac{e^{-j\alpha_1}}{T_{rpst1}} - \frac{e^{-j\alpha_2}}{T_{rpst2}}).I_{ser_1} + 2.I_o \\ &= \frac{1}{T_{ser}}(\frac{e^{-j\alpha_1}}{T_{rpst1}} - \frac{e^{-j\alpha_2}}{T_{rpst2}}).e^{-j\theta}I_{ser_2} + 2.I_o\end{aligned} \tag{15}$$

The primary side voltage of the shunt transformer and the sending side voltage are equal, i.e. $\overline{V}_{sh1} = \overline{V}_g$. Substituting Eqs.(15) and (9) into Eq. (14), we have:

$$\bar{V}_{ser2} = \frac{1}{T_{sh}T_{ser}}\left(\frac{e^{-j\alpha_1}}{T_{rpst1}} - \frac{e^{-j\alpha_2}}{T_{rpst2}}\right)e^{-j(\theta+\gamma)}\bar{V}_g - \ldots$$
$$\left(\frac{1}{T_{ser}^2}e^{-j2\theta}.2.Z_{rt} + \frac{1}{(T_{ser})^2}e^{-j2\theta}\left(\frac{e^{-j\alpha_1}}{T_{rpst1}} - \frac{e^{-j\alpha_2}}{T_{rpst2}}\right)^2 Z_{sh} + \right. \quad (16)$$
$$\left. Z_{se}\right).I_{ser_2} - \frac{1}{T_{ser}}e^{-j\theta}\left(\frac{e^{-j\alpha_1}}{T_{rpst1}} - \frac{e^{-j\alpha_2}}{T_{rpst2}}\right).Z_{sh}.2I_o$$

The magnetic current of RPSTs is:

$$I_o = \frac{1}{T_{sh}e^{j\gamma}(R_C \| jX_m + 2.Z_{sh})}V_g - \ldots$$
$$\frac{1}{R_C \| jX_m + 2.Z_{sh}}.\frac{1}{T_{ser}}\left(\frac{e^{-j\alpha_1}}{T_{rpst1}} - \frac{e^{-j\alpha_2}}{T_{rpst2}}\right)e^{-j\theta}.Z_{sh}I_{ser_2} \quad (17)$$

which R_C is shunt branch resistance of RPST and X_m is magnetizing reactance of RPST. Therefore, from Eqs. (16) and (17), we will have:

$$\bar{V}_{ser2} = \left(\frac{1}{T_{sh}T_{ser}}\left(\frac{e^{-j\alpha_1}}{T_{rpst1}} - \frac{e^{-j\alpha_2}}{T_{rpst2}}\right)e^{-j(\theta+\gamma)} - \ldots\right.$$
$$\frac{1}{T_{sh}T_{ser}}\left(\frac{e^{-j\alpha_1}}{T_{rpst1}} - \frac{e^{-j\alpha_2}}{T_{rpst2}}\right).\frac{2Z_{sh}e^{-j(\gamma+\theta)}}{R_C \| jX_m + 2.Z_{sh}}\Big)V_g - \ldots$$
$$\left(\frac{1}{T_{ser}^2}e^{-j2\theta}2.Z_{rt} + Z_{se} + \ldots\right. \quad (18)$$
$$\frac{1}{(T_{ser})^2}e^{-j2\theta}\left(\frac{e^{-j\alpha_1}}{T_{rpst1}} - \frac{e^{-j\alpha_2}}{T_{rpst2}}\right)^2 Z_{sh} - \ldots$$
$$\left.\frac{1}{(T_{ser})^2}\left(\frac{e^{-j\alpha_1}}{T_{rpst1}} - \frac{e^{-j\alpha_2}}{T_{rpst2}}\right)^2\frac{2(Z_{sh})^2e^{-j2\theta}}{R_C \| jX_m + 2.Z_{sh}}\right).I_{ser_2}$$

Supposing $T_{rpst_1} = T_{rpst_2} = T_{rpst}$, the impedance of the RPFC can be obtained by the following equation:

$$Z_{rpfc} = \frac{e^{-j2\theta}}{T_{ser}^2}.2.Z_{rt} + \frac{e^{-j2\theta}}{(T_{ser}T_{rpst})^2}(e^{-j\alpha_1} - e^{-j\alpha_2})^2 Z_{sh} \ldots$$
$$+Z_{se} - \frac{1}{(T_{ser}.T_{rpst})^2}.(e^{-j\alpha_1} - e^{-j\alpha_2})^2.\frac{2(Z_{sh})^2e^{-j2\theta}}{R_C \| jX_m + 2.Z_{sh}} \quad (19)$$

Thus, from Eqs. (18) and (19) we have:

$$\bar{V}_{ser2} = \left(\frac{e^{-j(\theta+\gamma)}}{T_{sh}.T_{ser}.T_{rpst}}(e^{-j\alpha_1} - e^{-j\alpha_2})\right.$$
$$\left.\frac{1}{T_{sh}.T_{ser}.T_{rpst}}(e^{-j\alpha_1} - e^{-j\alpha_2}).\frac{2Z_{sh}e^{-j(\theta+\gamma)}}{R_C \| jX_m + 2Z_{sh}}\right).V_g - Z_{rpfc}.I_{ser_2} \quad (20)$$

3.3 Effect of RPFC Installation on Sending Side Voltage

To evaluate the effect of the RPFC installation on the active and reactive power flow of the network, the sending side voltage variations due to presence of the RPFC are calculated. The relation between $\bar{V}_s$ and $\bar{V}_g$ is:

$$\bar{V}_s = \bar{V}_g + \bar{V}_{Ser2} \quad (21)$$

By changing the RPSTs angles, the injected voltage ($\bar{V}_{ser2}$) and consequently the power flow varies. Substituting $\bar{V}_{ser2}$ from Eq. (20) into Eq. (21) follows:

$$\bar{V}_s = \left(1 + \frac{1}{T_{sh}T_{ser}T_{rpst}}(e^{-j\alpha_1} - e^{-j\alpha_2})e^{-j(\theta+\gamma)} - \right.$$
$$\frac{1}{T_{sh}T_{ser}T_{rpst}}(e^{-j\alpha_1} - e^{-j\alpha_2})e^{-j(\theta+\gamma)} \quad (22)$$
$$\left.\times\frac{2.Z_{sh}}{R_C \| jX_m + 2.Z_{sh}}\right)V_g - Z_{rpfc}.I_{ser_2}$$

The secondary current of the series transformer can be calculated by the following equation:

$$I_{ser_2} = \frac{V_s - V_r}{Z_{Line}} \quad (23)$$

Thus, from Eqs. (23) and (22), we have:

$$\bar{V}_s = \left(\frac{Z_{Line}}{Z_{Line} + Z_{rpfc}}\right)\left(1 + \right.$$
$$\frac{1}{T_{sh}.T_{ser}.T_{rpst}}(e^{-j\alpha_1} - e^{-j\alpha_2})e^{-j(\theta+\gamma)} - \quad (24)$$
$$\frac{1}{T_{sh}.T_{ser}.T_{rpst}}(e^{-j\alpha_1} - e^{-j\alpha_2})e^{-j(\theta+\gamma)} \times$$
$$\left.\frac{2.Z_{sh}}{R_C \| jX_m + 2.Z_{sh}}\right).V_g + \left(\frac{Z_{rpfc}}{Z_{Line} + Z_{rpfc}}\right).V_r$$

Supposing $T_{eq} = T_{sh} \times T_{ser} \times T_{rpst}$, it can be found:

$$\bar{V}_s = \left(\frac{Z_{Line}}{Z_{Line} + Z_{rpfc}}\right)\left(1 + \frac{1}{T_{eq}}(e^{-j\alpha_1} - e^{-j\alpha_2})e^{-j(\theta+\gamma)}\right.$$
$$-\frac{1}{T_{eq}}(e^{-j\alpha_1} - e^{-j\alpha_2})e^{-j(\theta+\gamma)} \times \quad (25)$$
$$\left.\frac{2.Z_{sh}}{R_C \| jX_m + 2.Z_{sh}}\right).V_g + \left(\frac{Z_{rpfc}}{Z_{Line} + Z_{rpfc}}\right).V_r$$

The minimum and maximum of T_{eq} can be calculated using following equations:

$$T_{eq}^{\min} = T_{sh}^{\min} \times T_{ser}^{\min} \times T_{rpst} \quad (26)$$
$$T_{eq}^{\max} = T_{sh}^{\max} \times T_{ser}^{\max} \times T_{rpst} \quad (27)$$

3.4 Effect of RPFC Installation on Network Power Flow

The transmission line can be modeled by an inductance as follows:

$$Z_{Line} = Z_L = jX_L \quad (28)$$

The active power flowing through the line is:

$$P_{Line1} = \frac{|V_g|.|V_r|}{X_L} Sin(\theta_g - \theta_r) \quad (29)$$

Therefore, the active power flowing through the line after the RPFC installation is:

$$P_{Line2} = \frac{|V_S|.|V_r|}{X_L} Sin(\theta_S - \theta_r) \quad (30)$$

From Eqs.(29) and (30) the active power variation is:

$$\Delta P_{Line} = P_{Line\,2} - P_{Line\,1} \quad (31)$$

The reactive power flowing through the line before the RPFC installation is obtained by the following equation:

$$Q_{Line1} = \frac{|V_g|^2}{X_L} - \frac{|V_g|.|V_r|}{X_L} Cos(\theta_g - \theta_r) \quad (32)$$

After installation of the RPFC, we have:

$$Q_{Line2} = \frac{|V_S|^2}{X_L} - \frac{|V_S|.|V_r|}{X_L} Cos(\theta_S - \theta_r) \quad (33)$$

Therefore, the reactive power variation due to installation of the RPFC is:

$$\Delta Q_{Line} = Q_{Line\,2} - Q_{Line\,1} \quad (34)$$

The variations in active and reactive powers are dependent on each other. To show this coupling, the locus of active and reactive powers in the P-Q plane is illustrated in Fig. 3. The active and reactive power variations are confined to the circle area.

4 RPFC Operation Region

The RPFC equations presented in the previous section are used to calculate the operation region of the device. The RPFC and network parameters are shown in Tables 1 and 2.

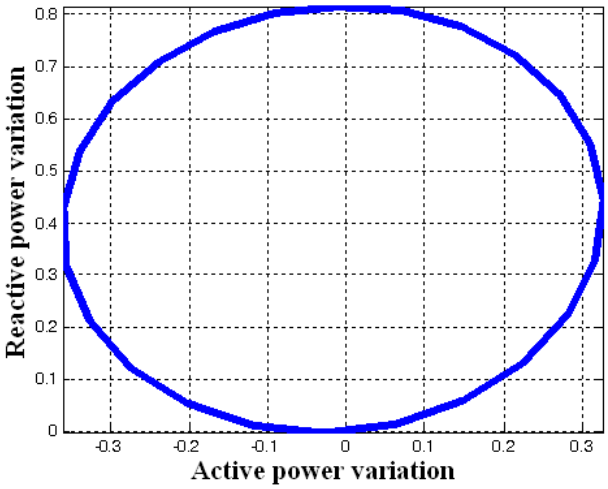

Fig. 3 Active and reactive power coupling of the RPFC.

Table 1 RPFC parameters.

Component	Power (MVA)	Primary voltage (kV)	Secondary voltage (kV)
RPST	250	25	25
Shunt transformer	500	400	25
Series transformer	500	50	125

Table 2 Transmission line parameters.

Parameter	Value
Sending end voltage ($\bar{V}_g$)	$400\angle 74.5\,kV$
Receiving end voltage ($\bar{V}_r$)	$400\angle 72.6\,kV$
Line impedance Z_L	0.032+j0.336 $\Omega.km^{-1}$
Line length	150 km
Base voltage	400 kV
Base power	1000 MVA

4.1 Limitations of Amplitude and Phase of Sending Side Voltage

The variations of amplitude as a function of the RPSTs phase shifts are shown in Fig. 4. The device operates as an ordinary RPFC when the tap-changer is located at its nominal place. In this case, amplitude varies from 0.91 to 1.1. Using the tap-changer, amplitude can be varied between 0.87 and 1.15.

The variations of phase are depicted in Fig. 4. Phase variations ranges from 69.25° to 78.84° for ordinary RPFC and from 67.44° to 80.55° for RPFC with tap-changing transformers. Therefore, the operation region of the RPFC can be extended using the tap-changing transformers.

4.2 Limitations of Active and Reactive Powers of the Line

When the tap-changing transformers are used, due to the variation of amplitude and phase, the ability of the RPFC for controlling the active and reactive powers increases compared to the ordinary RPFC. Fig. 5 shows the effect of the RPFC installation on the variation of the active and reactive power passed through the 400 kV line. Using the RPFC, the active power of the line can vary between -0.305 and 0.275 p.u. The rise in reactive power is up to 0.677 p.u. However, the RPFC with tap-changing transformers can give the active power a range from -0.423 to 0.392 p.u. and the reactive power a range from 0 to 1 p.u.

4.3 Comparison between RPFCs with Ordinary and Tap-Changing Transformers

In this section, based on the previously presented results, comparisons are made between the abilities and operational region of the RPFC with and without tap-changing transformers. Table 3 concludes the results of the previous section. It is clear that the ability to control

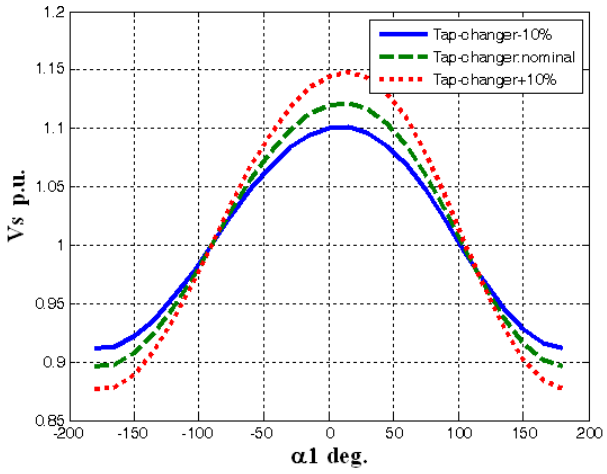

(a)

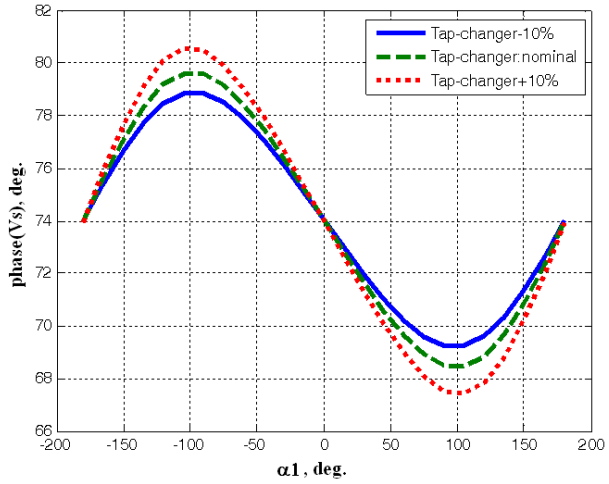

(b)

Fig. 4 (a) Amplitude and (b) phase as a function of α_1-α_2.

the active and reactive power of the line has increased up to 40% and 47%. Therefore, using tap-changing transformers without increasing the RPFC rating increases the operator flexibility to control the transmission network.

Because maximum transformer voltage variation due to the existence of the tap changer is assumed to be ±10% and considering parameters shown in Table 3, rotor voltage of both RPSTs rise up to 27.8 kV and the stator voltage rises up to 55.5 kV. Therefore, expanding the control region results in a rise in the voltage rating of the RPSTs. Temporary use of tap-changer to extend the operation region of a transmission line is permissible without increasing the RPST rating. The thermal capacity of the RPSTs limits the duration of this extended capability operation.

5 Simulation Results

A 400 kV line and an RPFC as shown in Fig. 6 are simulated using PSCAD/EMTDC software. A step up 230/400 kV and a step down 400/230 kV transformer are installed at sending and receiving sides of the line. A 150 km line connects the sending and receiving buses. The RPFC is installed at the HV side of the step up transformer. A 132 MVAr capacitor bank is connected to the primary side of the shunt transformer to supply the reactive power consumed by the RPFC. The RPFC is used to control the active power flow of the line. Table 3 shows the parameters used in the simulation. Also, Table 4 shows comparison between analytical and simulation results of RPFC with tap-changing transformers and Ordinary RPFC.

Table 3 Operation region of the RPFC with/without tap-changing transformers.

Variation of line power	Ordinary RPFC	RPFC with tap-changing transformers	Percentage of variation
Active power (p.u.)	-0.305 to 0.275	-0.423 to 0.392	+40%
Reactive power (p.u.)	0 to 0.677	0 to 1	+47%

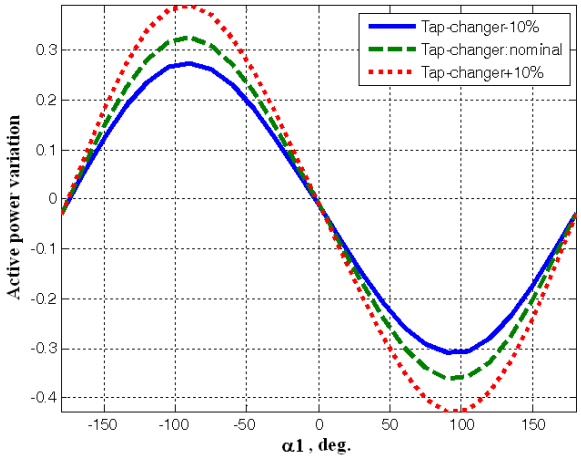

(a)

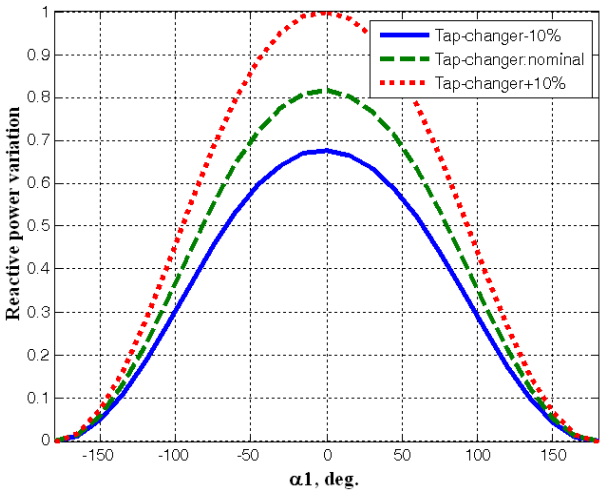

Fig. 5 Transmission line power after installation of the RPFC. (a) active and (b) reactive.

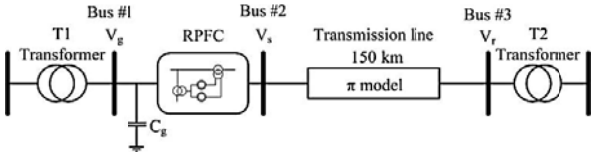

Fig. 6 The benchmark network for testing RPFC with tap-changing transformers.

Table 3 Parameters utilized in simulation.

Component	Value
Step up transformer T1	1500 MVA , 230/400 kV X=0.085 p.u. , R=0.002 p.u.
Step down transformer T2	1500 MVA , 400/230 kV X=0.085 p.u. , R=0.002 p.u.
Transmission line	Model: PI Line: 150 km , R=0.032 Ω/km X=0.336 Ω/km , B=3.375 Ω/km
RPFC	Shunt transformer: 500 KVA , 400/25kV, X=0.1 p.u Series transformer : 500 KVA , 50/125kV, X=0.1 p.u RPST: 250 MVA, 25 Kv, J=0.7267 s

Table 4 Comparison between analytical and simulation results.

Variation of line active power (p.u.)	Ordinary RPFC	RPFC with tap-changing transformers	Percentage of variation
Analytic results	-0.305 to 0.275	-0.423 to 0.392	+40%
Simulation results	-0.46 to 0.42	-0.57 to 0.532	+25%

5.1 Dynamic Operation of Ordinary RPFC

In normal conditions and without RPFC, 105 MW active power flows from the bus #2 to the bus #3. The reference power of the RPFC is set equal to 110 MW. At t=1 sec. the reference power increases to 130 MW. Fig. 7 depicts the active power variations of the line. The overshoot is damped in less than half a cycle and the new steady state operation point is reached. The amplitude of the voltage at buses #1 and 3 is shown in Fig. 8. The voltage transient oscillations are completely damped after two cycles.

5.2 RPFC Operational Region Limitation

To determine the operational limit of the system without using the tap-changer, the reference power has been raised. The system response to the rise of the active power is shown in Fig. 9. It is clear when the reference power is greater than 551.5 MW, the system is unstable. Fig. 10 indicates that the line voltage does not increase more than 5% which is the overvoltage standard limitation. Therefore, only the RPSTs angle limits the operation of the RPFC.

Before instability, the operation of the RPFC with and without tap-changer is quite similar. Fig. 11 demonstrates that before entering the unstable region the RPFC with tap-changer can raise the line active power up to 641.5 MW which is 16.3% more than the ability of an ordinary RPFC.

Fig. 12 displays the RMS value of the voltages of buses #1 and #3. The voltages of both buses satisfy the standard of the voltage limitations. Therefore, the upper bound of the line power is limited by the implicit limitation of the RPFC.

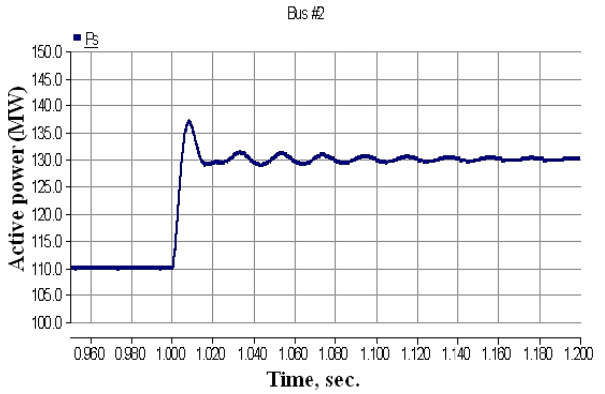

Fig. 7 Line active power after changing ordinary RPFC reference power.

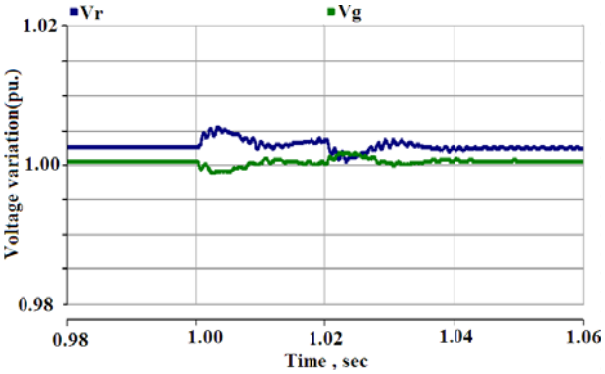

Fig. 8 RMS voltage of buses #1 and 3.

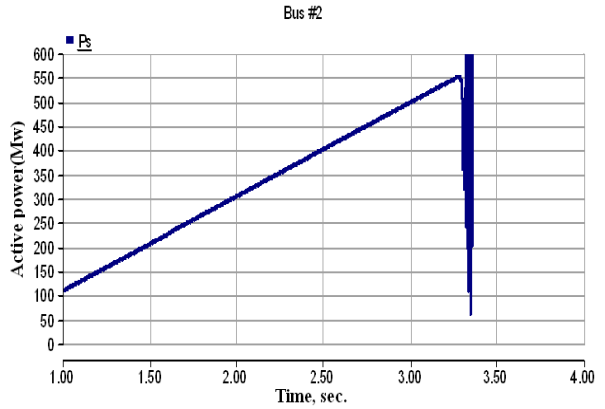

Fig. 9 The transmission line active power increased using RPFC.

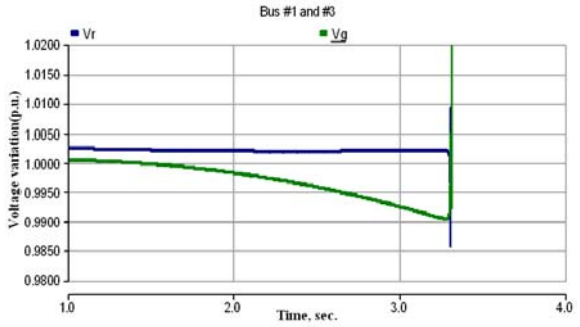

Fig. 10 The RMS voltage of the buses, #1 and 3.

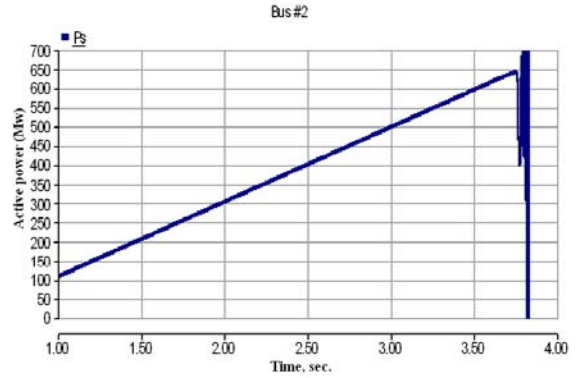

Fig. 11 The transmission line active power increased using RPFC with tap-changer.

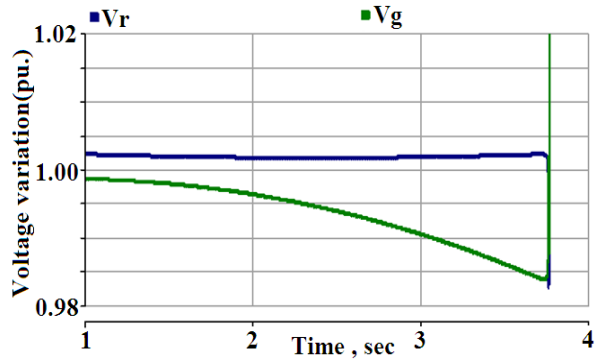

Fig. 12 Variation of RMS voltages of buses #1 and 3 due operation of the RPFC with tap-changer.

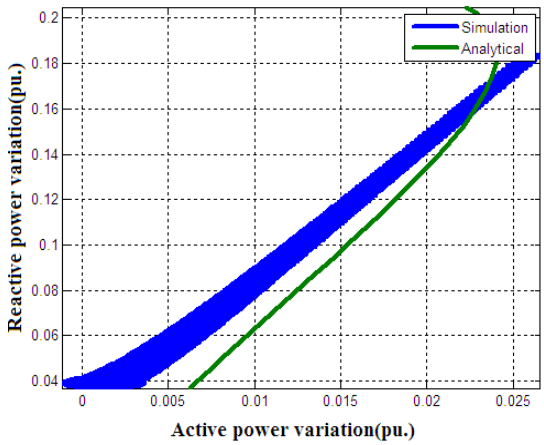

Fig. 13 Variation of active and reactive power of the RPFC.

5.3 Reactive Power Consumption

The active and reactive powers received by the RPFC shunt transformer are illustrated in Fig. 13. The active power received by the RPFC is injected into the network by the series transformer and supplies the internal losses. An increase in the received active power will result in a rapid rise of the reactive power. According to Fig. 13, the relation between the active and reactive power received by the RPFC from the network can be approximated using the following equation;

$$Q = 5.85 \times P + 29.9 \tag{35}$$

Consequently, for each unit of active power variation, the reactive power varies approximately 6 units. This indicates the RPFC consumes large amounts of reactive power. Increasing the capacity of the shunt capacitor bank can reduce the reactive power drawn from the network. However, this may cause overvoltage problem. The capacity of the capacitor bank used in the simulation is chosen based on the reactive power consumption when the RPFC operates at the midpoint of its active power control region (about 130 MW).

Increasing tap-changer of shunt and series transformers causes extending operation range of RPFC, but decreasing tap-changer of shunt transformer causes controlling voltage RPFC and protect from RPFC against network overvoltage. The control loop of the RPFC takes line active power as an input. By comparing line power with reference power, an error signal is generated. Therefore if configuration of the transformers varies, the changes will be appeared in the line active power and the input of the control algorithm will change. According to new inputs, the control algorithm generates new set point for RPFC operation. Moreover, because the RPST phase can be controlled continuously, the discreet steps in power flow caused by tap-changer variations can be compensated by RPFC control algorithm after a short time needed for change of RPST phase.

6 Conclusion

It has been shown that the operational region of the RPFC can be extended by using tap-changer in its series and shunt transformers. The increase in the operation region is calculated using the precise model of the system components. The RPFC is simulated on a 400 kV transmission line. The effects of the tap-changers operation on the device performance have been evaluated. It has been shown that the active power control region is expanded. The detailed modeling shows that by using the tap-changer the RPFC ability to control the active power of the transmission line increases about 40%. However, the simulations show that in the real case, the upper limit of the active power control ability increases 25% and the system is unstable after this point. Therefore, considering the temperature limitation of the components, the control region of the RPFC can extend using tap-changing transformers.

References

[1] Y. H. Song and A. T. Johns, *Flexible AC Transmission Systems (FACTS)*. London, U.K.: IEE Press, 1999.

[2] N. G. Hingorani and L. Gyugyi, *Understanding FACTS - Concepts and technology of Flexible AC Transmission Systems*, New York: IEEE Press, 2000.

[3] D. J. Gotham and G. T. Heydt, "Power Flow Control and Power Flow Studies for Systems with FACTS devices", *IEEE Trans. Power Sys*., Vol. 13, No.1, pp. 60-65, 1998.

[4] Y. Xiao, Y. H. Song and Y. Z. Sun, "Power Flow Control Approach to Power Systems with Embedded FACTS Devices", *IEEE Trans. Power Sys*., Vol. 17, No. 4, pp. 943-950, 2002.

[5] E. Acha, C. R. Fuerte- Esquivel, H. Ambriz-Perez and C. Angeles-Camacho, *FACTS, Modeling and Simulation in Power Networks*, John Wiley & Sons Ltd, England, pp. 1-28, Feb. 2004.

[6] E. V. Larsen, "Power flow control with rotary transformers", *United States Patent*, Patent Number: 5841267, Date of Patent: Nov. 24, 1998.

[7] E. V. Larsen, "Power flow control and power recovery with rotary transformers", *United States Patent*, Patent Number: 5953225, Date of Patent: Sep. 14, 1999.

[8] A. O. Ba, T. Pend and S. Lefebvre, "Rotary power-flow controller for dynamic performance evaluation- part I: RPFC modeling", *IEEE Transactions on Power Delivery*, Vol. 24, No. 3, pp. 1406-1416, July 2009.

[9] A. O. Ba, T. Pend and S. Lefebvre, "Rotary power-flow controller for dynamic performance evaluation- part II: RPFC application in a transmission corridor", *IEEE Transactions on Power Delivery*, Vol. 24, No. 3, pp. 1417-1425, July 2009.

[10] E. V. Larsen, "A classical approach to constructing a power flow controller", in Proc. *Power Engineering Society Summer Meeting*, Vol. 2, pp. 1192-1195, 1999.

[11] H. Fujita, S. Ihara, E. V. Larsen, E. R. Pratico and W. W. Price, "Modeling and dynamic performance of a rotary power flow controller", *in Proc. Power Engineering Society Meeting*, pp. 599-604, 2001.

[12] H. Fujita, S. Ihara, E. V. Larsen and W. W. Price, "Basic characteristics of a rotary power flow controller", *in Proc. Power Engineering Society Meeting*, pp. 1477-1482., 2000.

[13] M. Hosseini Abardeh and R. Ghazi, M. Tolue Khayami, "The operation analysis of rotary power flow controller (RPFC)", *Iranian Conference on Electrical Engineering*, 2011.

[14] M. Tolue Khayami, H. A. Shayanfar, A. Kazemi and M. Hosseini Abardeh, "The operation analysis of rotary power flow controller (RPFC) using detailed modeling", *Int. Power System Conf.*, 2012.

[15] M. Tolue Khayami, M. Hosseini Abardeh, H. A. Shayanfar and R. Ghazi, "The operation analysis and allocation of rotary power flow controller (RPFC) in the Khorasan transmission network", *Int. Power System Conf.*, 2011.

[16] M. Tolue Khayami, M. Hosseini Abardeh, H. A. Shayanfar and R. Ghazi, "Power system reliability enhancement using rotary power flow controller", *Int. Power System Conf.*, 2011.

Mohammad Tolue Khayami was born in 1975 in Mashhad, Iran. He received his B.Sc. in power engineering from Islamic Azad University (IAU), Bojnourd branch in 1998 and M.Sc. in power engineering from Iran University of Science and Technology (IUST), Tehran, Iran in 2001. He is now Ph.D. student at Department of Electrical Engineering, Science and Research Branch, Islamic Azad University, Tehran, Iran.

Heidarali Shayanfar received the B.Sc. and M.S.E. degrees in Electrical Engineering in 1973 and 1979, respectively. He received his Ph.D. degree in Electrical Engineering from Michigan State University, U.S.A., in 1981. Currently, he is a Full Professor in Electrical Engineering Department of Iran University of Science and Technology, Tehran, Iran. His research interests are in the Application of Artificial Intelligence to Power System Control Design, Dynamic Load Modeling, Power System Observability Studies, Voltage Collapse, Congestion Management in a Restructured Power System, Reliability.